Published in final edited form as:
Anal Chem. 2017 May 16; 89(10): 5484–5493. doi:10.1021/acs.analchem.7b00423.

Spectrophotometric Quantification of Peroxidase with *p*-Phenylenediamine for Analyzing Peroxidase-Encapsulating Lipid Vesicles

Ya Zhang[†,§], **Yannick R. F. Schmid**[‡], **Sandra Luginbühl**[†], **Qiang Wang**[§], **Petra S. Dittrich**[‡,iD], and **Peter Walde**[*,†,iD]

[†]Polymer Chemistry Group, Department of Materials, ETH Zürich, Vladimir-Prelog-Weg 5, CH-8093 Zürich, Switzerland [‡]Bioanalytics Group, Department of Biosystems Science and Engineering, ETH Zürich, Vladimir-Prelog-Weg 3, CH-8093 Zürich, Switzerland [§]Key Laboratory of Science and Technology of Eco-Textile, Jiangnan University, Wuxi 214122, Jiangsu China

Abstract

A spectrophotometric assay for the determination of horseradish peroxidase (HRP) in aqueous solution with *p*-phenylenediamine (PPD, benzene-1,4-diamine) as electron donor substrate and hydrogen peroxide (H_2O_2) as oxidant was developed. The oxidation of PPD by HRP/H_2O_2 leads to the formation of Bandrowski's base ((3*E*,6*E*)-3,6-bis[(4-aminophenyl)imino]cyclohexa-1,4-diene-1,4-diamine), which can be quantified by following the increase in absorbance at 500 nm. The assay was applied for monitoring the activity of HRP inside ≈180 nm-sized lipid vesicles (liposomes), prepared from POPC (1-palmitoyl-2-oleoyl-*sn*-glycero-3-phosphocholine) and purified by size exclusion chromatography. Because of the high POPC bilayer permeability of PPD and H_2O_2, the HRP-catalyzed oxidation of PPD occurs inside the vesicles once PPD and H_2O_2 are added to the vesicle suspension. In contrast, if instead of PPD the bilayer-impermeable substrate $ABTS^{2-}$(2,2′-azino-bis(3-ethylbenzothiazoline-6-sulfonate)) is used, the oxidation of $ABTS^{2-}$ inside the vesicles does not occur. Therefore, using PPD and $ABTS^{2-}$ in separate assays allows distinguishing between vesicle-trapped HRP and HRP in the external bulk solution. In this way, the storage stability of HRP-containing POPC vesicles was investigated in terms of HRP leakage and activity of entrapped HRP. It was found that pH 7.0 suspensions of POPC vesicles (2.2 mM POPC) containing on average about 12 HRP molecules per vesicle are stable for at least 1 month without any significant HRP leakage, if stored at 4 °C. Such high stability is beneficial not only for bioanalytical applications but also for exploring the kinetic properties of vesicle-

[iD]**ORCID**
Petra S. Dittrich: 0000-0001-5359-8403
Peter Walde: 0000-0002-0827-0545

[*]**Corresponding Author**: Phone: +41 44 632 0473. peter.walde@mat.ethz.ch.

Author Contributions
Y.Z. and Y.R.F.S. made equal contributions. The manuscript was written through contributions of all authors. All authors have given approval to the final version of the manuscript.

Notes
The authors declare no competing financial interest.

Europe PMC Funders Author Manuscripts

entrapped HRP through simple spectrophotometric absorption measurements with PPD as a sensitive and cheap substrate.

Horseradish peroxidase (HRP, EC 1.11.1.7) is a well-known heme-containing enzyme which is widely applied in bioanalytics, organic synthesis, and wastewater treatment.1–7 Following the oxidation of the heme group of HRP by added hydrogen peroxide (H_2O_2), the oxidized forms of HRP, compounds I and II, can oxidize relatively unspecifically a variety of different aromatic substrates. Some of these substrates can be applied for the spectrophotometric quantification of HRP. Basically, there are only two requirements for serving as chromogenic HRP substrate: (i) the absorption spectrum of the product(s) obtained must differ significantly from the absorption spectrum of the substrate and (ii) conditions must exist at which for a fixed H_2O_2 concentration the initial rate of substrate oxidation results in absorbance changes which depend (in the ideal case linearly), within a certain HRP concentration range, on the HRP concentration. These requirements are fulfilled, for example, in the case of $ABTS^{2-}$ (2,2′-azino-bis(3-ethylbenzothiazoline-6-sulfonate)), which can be analyzed at 414 nm (formation of the radical anion $ABTS^{\bullet-}$),8,9 or *o*-phenylenediamine (OPD, benzene-1,2-diamine), which is analyzed at a wavelength, λ, of 417 nm (formation of 2,3-diaminophenazine).10,11

The aim of the work was to explore the possibility of using *p*-phenylenediamine (PPD, benzene-1,4-diamine) as a chromogenic substrate of HRP for analyzing HRP entrapped in the aqueous interior of lipid vesicles (liposomes). The lipid we used was POPC (1-palmitoyl-2-oleoyl-*sn*-glycero-3-phosphocholine), and the aqueous solution with which the vesicles were formed, was a 50 mM potassium phosphate buffer of pH 7.0. Although PPD has already been, and is being, used as chromogenic substrate for determining the activity of ceruloplasmin, a multifunctional copper-containing protein,12–14 PPD was only scarcely applied as substrate of heme peroxidases, such as HRP,15 lactoperoxidase,16 or tomato peroxidase.17 For the purpose of our work with HRP-encapsulating POPC vesicles at pH 7.0, however, we considered PPD to have certain advantages over, for example, $ABTS^{2-}$ since PPD is a small molecule, uncharged at neutral pH and partially hydrophobic, but still water-soluble, and expected to be able to permeate across POPC bilayers. We thought that after adding H_2O_2 and PPD to a suspension of HRP-containing vesicles it is likely that both $H_2O_2$18 and PPD permeate relatively unhindered across the lipid bilayer of the vesicles so that they can reach the entrapped HRP and then react with it: oxidation of PPD and appropriate follow-up reactions. In this way the activity of the enzyme might be measurable spectrophotometrically inside intact vesicles without using fluorogenic substrates, therefore simplifying the analysis. This indeed turned out to be the case.

We first reinvestigated the use of PPD as chromogenic substrate for HRP and optimized the conditions so that low amounts of HRP can be quantified reliably by following the formation of the reaction product with absorption around 500 nm, which originates from Bandrowski's base (Figure 1).19–22

In a second step of the work, we prepared HRP-encapsulating POPC vesicles with average diameters of about 180 nm and investigated the stability of the entrapped HRP and its possible leakage from the vesicles during storage at 4 °C by using in addition to the PPD

method also the established spectrophotometric assay with $ABTS^{2-}$ (membrane impermeable). Knowing the storage stability of HRP-containing vesicles is an important requirement for their considerations in bioanalytical applications,23–32 as biomaterials,33 and possibly as HRP nanoreactors for biomedical applications,34 as suggested for vesicles prepared from amphiphilic block copolymers (polymersomes),35–37 or as sensory model compartment system and for fundamental studies of enzymes in volume-confined systems.

Experimental Section

Materials

PPD (*p*-phenylenediamine, 1,4-diaminobenzene, purum, > 99%), the diammonium salt of $ABTS^{2-}$ (2,2′-azino-bis(3-ethylbenzothiazoline-6-sulfonate)), cholic acid sodium salt (≥99%), Sepharose 4B, chloroform (stabilized with ethanol, 99.8%), ammonium thiocyanate (NH_4SCN, ≥99%), KH_2PO_4 (puriss p.a.), and K_2HPO_4 (≥98%) were purchased from Sigma-Aldrich. POPC (1-palmitoyl-2-oleoyl-*sn*-glycero-3-phosphocholine) was from Sigma-Aldrich (≥99%). Hydrogen peroxide (H_2O_2, 35%) and ferric chloride hexahydrate ($FeCl_3 \cdot 6H_2O$, ≥99%) were from Acros Organics; NaH_2PO_4 (≥98%) and methyl-t-butyl ether (MTBE, ≥ 99%) were from Fluka. All chemicals were used as obtained with the exception of PPD, which was purified by crystallization as follows. The slightly purple PPD product was first completely dissolved in ethanol (EtOH) by heating to 90 °C in an oil bath, followed by recrystallization in an ice bath. The obtained pink flocculent PPD crystals were then dissolved in benzene at 85 °C, followed by recrystallization at room temperature. The purified flocculent PPD crystals were snow-white and stored at room temperature in a brown bottle *in vacuo* before use. HRP (Horseradish peroxidase isoenzyme C, product code PEO-131, grade I, 278 U/mg, lot 2131616000, RZ (= A_{403}/A_{260}) > 3.1) was from Toyobo Enzymes (Japan), purchased through Sorachim SA, Switzerland. The HRP concentration was determined spectrophotometrically using $\varepsilon_{403} = 1.02 \times 10^5\ M^{-1}\ cm^{-1}$ as the molar absorption coefficient.38

Buffer Solutions

Two different buffer solutions were used. Buffer-1: 100 mM sodium phosphate, pH 7.0, prepared by dissolving NaH_2PO_4 in Milli-Q water, followed by pH adjustment with 2 M NaOH. Buffer-2: 50 mM potassium phosphate, pH 7.0, prepared from 61.5 mL of 1 M KH_2PO_4 and 38.5 mL of 1 M K_2HPO_4, filled up to 1 L with Milli-Q water.

UV−Visible Spectrophotometers

Absorption measurements in the ultraviolet (UV) and visible (vis) region of the spectrum were recorded at ≈25 °C with a Specord S 600 diode array instrument from Analytik Jena AG, Germany. For determining the HRP concentration in small volumes (below 0.1 mL), a NanoDrop ND1000 instrument from Thermo Fisher Scientific was used (about 5 μL required).

Mass Spectrometry (MS) Analysis

The MS analysis was carried out by the MS service of the Laboratory of Organic Chemistry at the Department of Chemistry and Applied Biosciences at ETH, using electrospray ionization (positive mode).

Sensitive Quantification of HRP in Bulk Aqueous Solution with PPD and H_2O_2

A HRP stock solution was prepared by dissolving 3.4 mg of HRP powder in 1 mL buffer-1, yielding 57.20 μM HRP (spectrophotometrically determined). This solution was further diluted two times (1:399, v/v) with buffer-1 to yield 357.5 pM HRP. This diluted solution was used within 1 day after preparation. A H_2O_2 stock solution (20 mM) was prepared by appropriate dilution with deionized water of a 35 wt % aqueous H_2O_2 solution (11.6 M). For each series of reactions, a PPD stock solution (40 mM) was freshly prepared by dissolving 4.32 mg of PPD in 1 mL of buffer-1.

The activity measurements were carried out at 25 °C in a 1 cm quartz cuvette (from Hellma). The changes in the absorption spectrum were recorded as a function of time. For each reaction, between 0 and 279.7 μL of the HRP stock solution was first added to 678.8−958.5 μL of phosphate buffer solution (pH 7.0) to yield a total volume of 958.5 μL. After the addition of 37.5 μL of the 40 mM PPD stock solution, the reaction was initiated by the addition of 4.0 μL of the 20 mM H_2O_2 stock solution, followed by a quick gentle shaking. Briefly, for assaying HRP in a concentration range between 10 and 100 pM at 25 °C, the following reaction conditions were found to be appropriate: [PPD] = 1.5 mM, [H_2O_2] = 80 μM. The reaction was monitored every minute for the first 30 min after H_2O_2 addition. One example for the first 10 min is shown in Figure 2. A plot of A_{500} (the absorbance at the isosbestic point, λ_{iso}) vs time showed that for 10−100 pM HRP the increase in A_{500} with time is linear during the first 10 min (Figure S-1). Therefore, A_{500} measured after 10 min was used for preparing a calibration curve with known amounts of HRP (Figure 3).

Preparation of HRP-Encapsulating Large Unilamellar POPC Vesicle (LUV_{200}) Suspensions

HRP-containing POPC vesicles were prepared by first hydrating a dry POPC film with an aqueous HRP solution, followed by polycarbonate membrane extrusion39 and size exclusion chromatography.40,41 Details of the preparation steps are given in the Supporting Information, illustrated in Figure S-2.

DLS Analysis of the Vesicle Fractions

Dynamic light scattering (DLS) measurements were carried out with a ZetaSizer Nano from Malvern by using disposable polystyrene semimicro cuvettes from BRAND with a path length of 1 cm.

Quantification of POPC in the Vesicle Fractions

The Stewart assay was employed to determine the POPC content of the vesicle fractions, 42,43 see the Supporting Information and Figure S-3.

Solubilization of POPC LUV_{200} with Sodium Cholate

The addition of sodium cholate to HRP-encapsulating POPC LUV_{200} leads to a transformation of the vesicles into mixed POPC-cholate vesicles and mixed cholate-POPC micelles,44 with a concomitant HRP release. For finding a suitable minimal amount of cholate for solubilizing the vesicles, POPC vesicles were prepared in the same way as described above but without HRP in the hydration solution (including extrusion and size exclusion chromatography). The main chromatographic fraction of this "empty" POPC LUV_{200} preparation (fraction 17) was then exposed to different cholate concentrations, and the turbidity was measured between 400 and 600 nm, see Figure S-4a. A cholate concentration of 8.0 mM was found to reduce the turbidity to baseline level with a HRP activity decrease of about 10%, see the Supporting Information (Figure S-4b).

HRP Activity of the Vesicle Fractions Measured with $ABTS^{2-}/H_2O_2$

Stock Solutions—The stock solutions were made as follows: $ABTS^{2-}$, 10 mM in buffer-2 (freshly prepared); H_2O_2, 20 mM in buffer-2 (freshly prepared); and sodium cholate, 200 mM in buffer-2.

Calibration Curves with Free HRP—Two calibration curves were prepared: (i) without sodium cholate and (ii) with 8.0 mM sodium cholate, see the Supporting Information (Figure S-5).

Intact HRP-Encapsulating Vesicles (No Cholate Addition)—A volume of 100 μL of the $ABTS^{2-}$ stock solution was added to 880 μL of buffer-2, followed by addition of 10 μL of vesicle fraction. The reaction was started by adding 10 μL of the H_2O_2 stock solution. Total volume: 1.0 mL, $[ABTS^{2-}]$ = 1.0 mM, $[H_2O_2]$ = 0.2 mM, 25 °C. The absorption spectrum was recorded every 15 s for the initial 150 s. As an example, the changes in the spectrum caused by the addition of vesicle fraction 16 are shown in Figure S-6a.

Solubilized HRP-Encapsulating Vesicles (After 8.0 mM Cholate Addition)—A volume of 100 μL of the $ABTS^{2-}$ stock solution was added to 840 μL of buffer-2, followed by addition of 10 μL of vesicle fraction and 40 μL of cholate stock solution. The reaction was started by adding 10 μL of the H_2O_2 stock solution. Total volume: 1.0 mL, [ABTS] = 1.0 mM, [cholate] = 8.0 mM, $[H_2O_2]$ = 0.2 mM, 25 °C. The absorption spectrum was recorded every 15 s for the initial 150 s. As an example, the changes in the spectrum caused by the addition of vesicle fraction 16 are shown in Figure S-6b.

Initial $ABTS^{2-}$ Oxidation at Fixed HRP and H_2O_2 and Variable $ABTS^{2-}$ Concentrations ("Michaelis-Menten Kinetics")

The initial rate of $ABTS^{2-}$ oxidation was measured in buffer-2 with 1.0 nM HRP, 0.2 mM H_2O_2, and $ABTS^{2-}$ concentrations varying between 0.05 and 1.80 mM (Figure S-7). The reactions were carried out in a similar way as described above. The initial rate was determined from the slope of the A_{414} vs time curve during the first 100 s after starting the reaction by H_2O_2 addition. The experimental data were fitted with the Michaelis−Menten equation by using the OriginPro software (version 8.5.0. SR1, from OriginLab Corporation).

HRP Activity of the Vesicle Fractions Measured with PPD/H_2O_2

Compared to the elaborated conditions for the quantification of HRP with PPD in bulk aqueous solution (see above and Figures 2 and 3), the assay conditions were adjusted for the same type of buffer (buffer-2) and for the same substrate concentration as used for the activity measurements with $ABTS^{2-}$, i.e., 1.0 mM PPD and 0.2 mM H_2O_2.

Stock Solutions—The stock solution were made as follows: PPD, 10 mM in buffer-2 (freshly prepared); H_2O_2, 20 mM in buffer-2 (freshly prepared); sodium cholate, 200 mM in buffer-2.

Calibration Curves with Free HRP—Two calibration curves were prepared: (i) without sodium cholate and (ii) with 8.0 mM sodium cholate, see the Supporting Information (Figure S-8).

Intact HRP-Encapsulating Vesicles (No Cholate Addition)—A volume of 100 μL of the PPD stock solution was added to 880 μL of buffer-2, followed by addition of 10 μL of vesicle fraction. The reaction was started by adding 10 μL of the H_2O_2 stock solution. Total volume: 1.0 mL, [PPD] = 1.0 mM, [H_2O_2] = 0.2 mM, 25 °C. The absorption spectrum was recorded every 15 s for the initial 150 s. As an example, the changes in the spectrum caused by the addition of vesicle fraction 15 are shown in Figure S-9a.

Solubilized HRP-Encapsulating Vesicles (after 8.0 mM Cholate Addition)—A volume of 100 μL of the PPD stock solution was added to 840 μL of buffer-2, followed by addition of 10 μL of vesicle fraction and 40 μL of the cholate stock solution. The reaction was started by adding 10 μL of the H_2O_2 stock solution. Total volume: 1.0 mL, [PPD] = 1.0 mM, [cholate] = 0.2 mM, [H_2O_2] = 0.2 mM, 25 °C. The absorption spectrum was recorded every 15 s for the initial 150 s. As an example, the changes in the spectrum caused by the addition of vesicle fraction 15 are shown in Figure S-9b.

Initial PPD Oxidation/Trimerization at Fixed HRP and H_2O_2 and Variable PPD Concentrations

The initial rate of the formation of Bandrowski's base from PPD was measured in buffer-2 with 0.5 nM HRP, 0.2 mM H_2O_2, and PPD concentrations varying between 0.05 and 1.50 mM (Figure 4). The reactions were carried out in a similar way as described above. The initial rate of formation of Bandrowski's base was determined from the slope of the A_{500} time curve recorded during the first 100 s after starting the reaction by H_2O_2 addition. The experimental data were fitted with the Michaelis−Menten equation by using the OriginPro software mentioned above.

Results and Discussion

Optimal Assay Conditions for Quantifying Low Amounts of HRP in Bulk Solution with PPD

The following conditions were found to be ideal for quantifying picomolar concentrations of HRP with PPD in aqueous solution: 1.5 mM PPD, 80 μM H_2O_2, pH 7.0 (100 mM sodium phosphate buffer buffer-1), 25 °C, 10 min reaction time, see Experimental Section. In the

presence of HRP and H_2O_2, the initially colorless PPD solution (absorption maximum at ≈280−300 nm, depending on pH)45–47 transforms into a purple solution (λ_{max} ≈ 520 nm), see Figure 2 for the changes occurring in the absorption spectrum during the first 10 min with 20 pM HRP. Without HRP, the spectral changes are the same, but they occur much slower (Figure S-1). Therefore, nonenzymatic PPD oxidation15 does not hinder HRP quantification. In Figure 3, the absorbance at 500 nm, A_{500}, after 10 min is shown for HRP concentrations varying between 10 pM and 0.1 nM. There is a clear linear relation between A_{500} (measured after 10 min) and the HRP concentration. Independent of whether HRP is present or not, the product obtained from PPD under the conditions used at pH 7.0, at least during the initial phase of the reaction, is Bandrowski's base,20,22 see Figure 1 and Figure S-10. Depending on the pH, Bandrowski's base exists in its neutral form, abbreviated as BB, or in its mono- or diprotonated form, BBH^+ and $BBH2^{2+}$, respectively. The reported pK_a value of BBH^+, protonation occurring at one of the imino-nitrogens, is 7.4.20 The pK_a value of BBH_2^{2+} must be below 5, because in aqueous solution between pH 5 and pH 12 the absorption spectrum shows the presence of two main components only (two isosbestic points at 500 nm and about 405 nm).20 Therefore, BBH^+ and BB are the dominating species obtained with HRP and H_2O_2 at the pH 7.0 assay conditions we used (Figure 1).46 The absorption maximum of BBH^+ is at 530−540 nm (with a molar absorption coefficient, $\varepsilon_{530-540}$ = 1.288 × 10^4 M^{-1} cm^{-1}).20 For BB, λ_{max} = 460 nm and ε_{460} = 1.288 × 10^4 M^{-1} cm^{-1}),20 exactly the same value as $\varepsilon_{530-540}$ of BBH^+. At λ_{iso} = 500 nm, ε_{500} = 11 090 M^{-1} cm^{-1}.48 In order to eliminate changes in absorbance caused by small changes in pH, the formation of Bandrowski's base in the elaborated assay was analyzed at this upper isosbestic point, i.e., at 500 nm, see Figure 3. As an example, A_{500} = 0.1 in Figure 3 means that within the first 10 min of reaction 9.0 μM Bandrowski's base formed, i.e., 27 μM PPD (and 27 μM H_2O_2) are consumed, corresponding to 1.8% of the initially present 1.5 mM PPD (and 34% of the added H_2O_2). The sensitivity of the PPD assay for determining HRP is comparable to the sensitivity and conditions of the assay using OPD.11 The main difference between the two assays is the different wavelengths at which product formation is monitored, 500 nm in the case of PPD and 417 nm for OPD.11 The latter wavelength is close to the one which is usually also used in the case of $ABTS^{2-}$.8,9

Determination of Apparent K_M and k_{cat} Values for PPD and HRP at pH 7.0

The PPD assay conditions can easily be adjusted for quantifying HRP above 0.1 nM (Figure S-8a). In Figure 4, the initial rate of the formation of Bandrowski's base, v_{in}, is plotted for different PPD concentrations between 0.05 and 1.50 mM at [H_2O_2] = 0.2 mM and [HRP] = 0.5 nM (pH 7.0, 25 °C). At [PPD] = 0.05−0.2 mM, the rate increased almost linearly with increasing PPD concentration, while for 0.2 mM < [PPD] < 1.5 mM, there was still an increase in the rate but clearly nonlinearly. The entire reaction is rather complex: (a) H_2O_2 is also a substrate of HRP (K_M (H_2O_2) ≈ 12 μM),49 (b) the oxidation of PPD is expected to follow a ping-pong mechanism (ordered two substrates two products) with two subsequent one electron steps,50 and (c) the formation of Bandrowski's base involves three PPD molecules and fast nonenzymatic follow-up reactions. It is likely that HRP is only involved in the oxidation of PPD to the *p*-phenylenediamine radical, $PPD^{\bullet}$. The subsequent oxidation and coupling steps may then occur without direct involvement of HRP, e.g., through disproportionation reactions and direct oxidations with H_2O_2 and via Michael-type

nucleophilic additions of PPD to intermediate diimines, see the suggested mechanism in Scheme S-1. The data in Figure 4 were fit with the Michaelis–Menten equation ($v_{in} = v_{max}$ [PPD]/(K_M + [PPD]), v_{max} being the maximal rate, whereby v_{max}/[HRP] = k_{cat}, the turnover number; solid line). This analysis yields apparent values for K_M and k_{cat} for PPD at pH 7.0 and 25 °C (at 0.2 mM H_2O_2) of 0.92 ± 0.09 mM (K_M) and 1064 ± 55 s^{-1} (k_{cat}).

Because of the discussed complexity of the reaction, it is somewhat surprising that the formation of Bandrowski's base with HRP follows Michaelis–Menten kinetics. The determined apparent values of K_M and k_{cat} have to be taken cautiously. In the case of the reducing substrate $ABTS^{2-}$, the situation is a bit different, since the rate of reaction is determined by analyzing the formation of $ABTS^{\bullet-}$, i.e., no nonenzymatic follow-up reactions are involved in the spectrophotometric analysis, as long as the disproportionation of two $ABTS^{\bullet-}$ species into $ABTS^{2-}$ and ABTS can be ignored.8 For the sake of a direct comparison, we also determined the apparent K_M and k_{cat} values for $ABTS^{2-}$ at pH 7.0 and 25 °C with [HRP] = 1.0 nM, [H_2O_2] = 0.2 mM, and [$ABTS^{2-}$] = 0.05−1.80 mM, see Figure S-7. The values obtained are 0.96 ± 0.13 mM (apparent K_M) and 160 ± 10 s^{-1} (apparent k_{cat}). These values are similar to previously determined values for HRP isoenzyme C and $ABTS^{2-}$ under comparable experimental conditions: 0.64 ± 0.06 mM and 45.5 ± 2.0 s^{-1} (pH 7.0, 25 °C, Rodriguez-Lopóez et al., 2000);50 0.44 ± 0.03 mM and 226 ± 14 s^{-1} (pH 6.0, 25 °C, Ryabov et al., 1999);51 0.24 ± 0.01 mM and 211 ± 7 s^{-1} (pH 6.0, 25 °C; Grotzky et al., 2013).52 With this comparison, it is clear that at neutral pH values and 25 °C the apparent k_{cat} value for the oxidation of PPD with HRP/H_2O_2 is at least about 4–5 times higher than the apparent k_{cat} value for $ABTS^{2-}$.

Preparation of HRP-Encapsulating POPC LUV_{200}

The general methodology used for the preparation of HRP-containing POPC vesicles is basically the same as described previously for encapsulating HRP in vesicles formed from a mixture of egg yolk phosphatidylcholine (egg PC), 1,2-dimyristoyl-*sn*-glycero-3-phospho-(1′-*rac*-glycerol sodium salt (DMPG), and cholesterol (4:1:5, molar ratios),40 or for encapsulating α-chymotrypsin in POPC vesicles,41,53 see the Supporting Information (Figure S-2). In short, a thin film of POPC was first formed inside a round-bottom flask made from silicate glass. This film was hydrated with a 50 mM potassium phosphate buffer solution of pH 7.0 (buffer-2) containing HRP at a total final concentration of 31 μM to obtain a multilamellar vesicle suspension of 20 mM POPC. In a next step, the size and the lamellarity of the vesicles were decreased by polycarbonate membrane extrusion (final extrusions through a membrane with a nominal pore diameter of 200 nm), yielding a suspension of mainly large unilamellar vesicles, abbreviated as LUV_{200} (with the subscript "200" the nominal pore diameter of the membranes used for the final extrusions is specified).39 In the absence of attractive interactions between HRP and POPC, only a very small portion of the HRP molecules used during the preparation is expected to be entrapped inside the LUV_{200} by this procedure (<5%). The calculated trapped aqueous volume of LUV_{200} with a diameter of 200 nm is 6.7 μL $\mu$$mol^{-1}$ POPC,54 i.e., 13.7 μL mL^{-1} (= 1.37 vol %) for 20 mM POPC (= 20 μmol POPC mL^{-1}). Nonentrapped HRP was separated from the HRP-encapsulating vesicles by size exclusion chromatography (Sepharose 4B), whereby the length of the column was chosen such, that complete separation could be achieved, see

Figure 5. Great care was taken in performing this separation since incomplete removal of nonentrapped HRP may lead to wrong conclusions from measurements carried out with fractions of HRP-encapsulating vesicles (see below).55 Figure 5a shows for each fraction A_{275} (protein band) and A403 (Soret band of the heme group) vs fraction number. For the vesicle fractions (numbers 15–21), the measured values A_{275} and A_{403} do not only reflect true light absorption but mainly originate from scattered light which did not reach the detector (turbidity caused by the vesicles). The HRP activity in the vesicle fractions was measured by adding a small volume of the fractions to either an assay solution of $ABTS^{2-}$ (1.0 mM) and H_2O_2 (0.2 mM) (Figure 5b) or to an assay solution of PPD (1.0 mM) and H_2O_2 (0.2 mM) (Figure 5c), see also Table S-1. For both substrates, the HRP activity was also measured in the presence of sodium cholate (8.0 mM) to destroy the vesicles and to release vesicle-entrapped HRP. By taking into account appropriate calibration curves prepared with known amounts of HRP (see Figure S-5b for $ABTS^{2-}$ and Figure S-8b for PPD), the activity measurements carried out in the presence of cholate provided information about the total amount of active HRP in each vesicle fraction. The corresponding values are given for the determinations with both substrates in Figure 5b,c (*y*-axis on the right-hand side). The quantifications agree quite well with each other and correlate qualitatively with A_{275} and A_{403}. The fraction with the highest HRP activity (or content) was the one with the highest A_{275} and A_{403} values, i.e., fraction 16. For the HRP activity measurements of the vesicle fractions carried out without cholate, a clear substrate selectivity exists, which is due to the different POPC bilayer permeabilities of the two substrates; while there was only a minor extent of $ABTS^{2-}$ oxidation, the oxidation of PPD to Bandrowski's base occurred readily, although the reaction was slower than in the presence of 8.0 mM cholate, see also Figure S-9.

The total amount of POPC applied onto the Sepharose 4B column and the amount of POPC in each vesicle fraction was determined with the Stewart assay42,43 by taking into account an appropriate calibration curve (Figure S-3). The results are shown in Figure 5d and Table S-1. While the entire amount of applied POPC was found to elute in the pooled vesicle fractions 15–21 (≈6.0 μmol), these vesicle fractions contained only 1.25% of the applied amount of HRP (200 pmol of 16 nmol, Table 1), which is in the range of the expected amount, see above. With the chosen method of vesicle preparation, the vast majority of the HRP molecules will not be trapped inside the vesicles but remains in bulk solution, eluting in fractions 30–45 (Figure 5a and Figure S-11). Therefore, an efficient separation of nonentrapped enzyme for the preparation of enzyme-encapsulating vesicles is absolutely essential for making sure that any detected enzyme activity in the prepared vesicle suspension is caused by entrapped enzyme molecules and not by enzyme molecules which are present in bulk solution.

Since for the analysis of the vesicle fractions with $ABTS^{2-}$ *without* cholate (Figure 5b, empty symbol), $ABTS^{\bullet-}$ formation always occurred to a small extent, we tested the stability of $ABTS^{2-}$ (and PPD) in the presence of "empty" POPC vesicles, prepared in the same way as with HRP and passed through a Sepharose 4 B column. Somewhat surprisingly, we found that for both substrates their oxidation is promoted by the vesicles in the presence of H_2O_2 (0.2 mM) in a vesicle concentration-dependent manner, see Figures S-12a and S-13a. The extent of oxidation in the case of $ABTS^{2-}$ (Figure S-12b) agrees well with the extent of

oxidation observed for the fractions with the vesicles containing encapsulated HRP (fractions 15–21 in Figure 5b). Therefore, the observed oxidation of $ABTS^{2-}$ in the case of HRP-encapsulating vesicles (measurements *without* cholate addition, Figure 5b, empty symbol) is due to the vesicles and not due to HRP. For PPD, the background activity caused by "empty" POPC vesicles and H_2O_2 (0.2 mM) is shown in Figure S-13b. This "activity" was much smaller than the activity measured with the fractions containing vesicles-entrapping HRP (Figure 5c, open symbol). The reason for the effect of empty POPC vesicles on the stability of $ABTS^{2-}$ or PPD in the presence of H_2O_2 is not clear at the moment but certainly deserves detailed future investigations. It may be due to a phospholipid-mediated activation of H_2O_2, which leads to an increased oxidative power of the added H_2O_2.56,57

Overall, the data clearly show that PPD which is added to HRP-encapsulating POPC LUV_{200} at pH = 7.0 can reach the vesicle-trapped enzyme, while the permeability of the POPC bilayer for $ABTS^{2-}$ is so low that $ABTS^{2-}$ cannot cross the membrane. The latter conclusion about $ABTS^{2-}$ is in agreement with previous observations for vesicles formed from egg lecithin,58 or DPPC.59 For the best of our knowledge, no permeability literature data is available for PPD. However, a high POPC bilayer permeability of PPD at pH 7.0 is expected since (i) the majority of the PPD molecules is present in their neutral form,46 and (ii) the reported permeability coefficient of the neutral form of the related compound tyramine (= 4-(2-aminoethyl)phenol) for DOPC/DOPA (96:4, mol ratio) LUV_{100} bilayers at 25 °C is high, $P = 1.74 \pm 1.05 \times 10^{-2}$ cm s^{-1}.60 Molecules with such a high value of P are expected to be taken up by the vesicles very rapidly, see Figure S-14.

The situation with the HRP-encapsulating POPC LUV_{200} and externally added H_2O_2, PPD, and $ABTS^{2-}$ is illustrated in Figure 6: the selective oxidation and trimerization of PPD inside the vesicles to yield Bandrowski's base.

Quantification of HRP-Encapsulating POPC LUV_{200}

As already mentioned above, all vesicle fractions were analyzed for content of POPC and content of active HRP, see Figure 5 and Table S-1. In order to further quantify the HRP loading of the vesicles, size determinations were carried out by dynamic light scattering measurements, yielding a hydrodynamic diameter (D_h) of about 180 nm for the vesicles eluting in fraction 16 (Table 1), the one with the highest POPC and HRP contents, and for the vesicles of the pooled fractions (15–21), all values with a polydispersity of less than 0.1, see Table S-2.

For fraction 16, the POPC concentration was 2.17 mM and the overall HRP concentration was 92 nM; for the pooled vesicle fractions, the values were 1.10 mM (POPC) and 37 nM (HRP), see Table 1. Assuming uniform spherical size and unilamellarity of LUV_{200}, an average POPC headgroup area of 0.72 nm^2 and a bilayer thickness of 3.7 nm,61,62 one can calculate that one 180 nm POPC vesicle is composed of about 278 000 POPC molecules and has an internal aqueous volume of 2.88×10^{-18} L (= 2.88 aL). Furthermore, the calculated concentration of vesicles in fraction 16 was 7.8 nM, which means that each vesicle on average contained ≈12 HRP molecules, corresponding to 6.8 μM HRP inside the vesicles, see Table 1 for details. This calculated value is lower than the HRP concentration used for dispersing the POPC molecules (62 μM or 31 μM after dilution, see the Experimental

Section). We did not attempt to increase the entrapment efficiency, for example, by using freeze–thawing cycles53 or by applying another method.54

Stability of HRP-Encapsulating POPC LUV_{200}

The combined use of both substrates allows an easy spectrophotometric monitoring of the stability of HRP entrapped inside POPC vesicles (with PPD) and of the leakage of HRP from the vesicles (with $ABTS^{2-}$), for example, during storage. Knowing such stability is essential for applications of HRP-containing vesicles. Therefore, the storage stability of HRP-encapsulating vesicles was investigated by using the fraction with the highest HRP activity (fraction 16, Figure 5, Table 1). This vesicle suspension (fraction 16) was stored at 4 °C, and the HRP activity was measured from time to time at 25 °C with $ABTS^{2-}/H_2O_2$ in the absence and in the presence of 8.0 mM cholate (Figure 7). A comparison was made with the stability of free HRP dissolved in buffer-2 at 1.0 nM. Similarly to free HRP (3 in Figure 7), the LUV_{200}-entrapped HRP was stable for at least 31 days (2 in Figure 7) without significant enzyme leakage (1 in Figure 7). The stability of HRP-encapsulating POPC LUV_{200} is much higher than the one reported by Suita et al.40 for HRP-encapsulating LUV_{1000} formed from egg PC, DMPG, and cholesterol (4:1:5, molar ratios) at 4 °C and pH = 7.2 (10 mM Mops-buffered saline). Whether this higher stability of HRP POPC LUV_{200} is due to differences in the types of lipids used or in the size and/or lamellarity is not clear.

Application of the PPD Assay for Characterizing HRP-Encapsulating POPC LUV_{200}

The preparation of HRP-encapsulating POPC LUV_{200} with the procedure described above was carried out three times. The reproducibility is high, which is at least partially due to the high stability of HRP. For a second preparation, the chromatogram for the separation of HRP-containing vesicles from free HRP is shown in Figure S-15 and the results of the quantification of some of the vesicle fractions are given in Table S-3. The fraction with the highest HRP content was used at a fixed overall concentration of HRP (0.5 nM) for PPD activity measurements with varying concentrations of PPD (0.05–1.50 mM) and a fixed H_2O_2 concentration (0.2 mM). The measured initial rate of formation of Bandrowski's base is shown in Figure S-16. A fit of the experimental data with the Michaelis–Menten equation yielded apparent values for K_M and k_{cat} of 0.79 ± 0.07 mM and 720 ± 33 s^{-1}.63 Both of these values are in the same order of magnitude as the values for the free enzyme. Although it is not immediately clear why the data shown in Figure S-16 obey Michaelis–Menten kinetics and what the determined apparent values mean, they are taken as interesting preliminary observation for further more detailed investigations toward a better understanding of enzyme-catalyzed, vesicle-confined reactions.64 Ultrafiltration experiments showed that the reaction product, Bandrowski's base, did not remain inside the vesicles but leaked out (Figure S-17). Future systematic measurements should show whether the measured reaction rates reflect the influence of the permeability barrier provided by the POPC bilayer, or whether they are related to the enzyme concentration inside the vesicles (about 4.2 μM, Table S-3), which is much higher in the case of the reaction studied in bulk solution (0.5 nM, Figure 4). The POPC-HRP/H_2O_2/PPD system appears to be an ideal sensitive model system, with which fundamental questions concerning enzymatic reactions inside submicrometer-sized compartments can be answered. Such studies are considered complementary to previous studies on the hydrolysis of benzoyl-L-tyrosine-*p*-nitroanilide

(Bz-Tyr-pNA) with α-chymotrypsin-encapsulating POPC LUV_{100} 41 or DOPC-LUV_{200} 65 (DOPC = 1,2-dioleoyl-*sn*-glycero-3-phosphocholine); in the case of Bz-Tyr-pNA, the bilayer permeability coefficient is lower ($\approx 10^{-7}$ cm s^{-1})41,65 than for PPD ($\approx 10^{-2}$ cm s^{-1}, see above).

Conclusions and Outlook

PPD is a sensitive substrate for quantifying HRP with high reproducibility in aqueous solution and in vesicle suspensions in the presence of H_2O_2 at nanomolar or even subnanomolar concentrations. The oxidation of PPD by HRP/H_2O_2 results in the rapid formation of Bandrowski's base, which is the linear trimer of PPD with an isosbestic point at 500 nm and a molar absorbance of ε_{500} = 11 090 $M^{-1}cm^{-1}$.48 PPD is particular useful for analyzing the activity of HRP inside phospholipid vesicles. Using HRP-encapsulating extruded POPC vesicles, POPC LUV_{200}, with PPD and the alternative electron donor substrate $ABTS^{2-}$, it could be demonstrated that the entrapped enzyme shows a substrate selectivity which is based on significant differences in the POPC bilayer permeability of the two substrates. While the POPC bilayer is highly permeable for PPD, it is impermeable for $ABTS^{2-}$. Since the storage stability of HRP-encapsulating POPC LUV_{200} is very high,these vesicles are an interesting model system for studying basic aspects of the activity of enzymes inside confined volumes upon external addition of substrates.64 Furthermore, the high stability of HRP-encapsulating POPC LUV_{200} allows using them as sensory tools for bioanalytical applications. The enzymes are protected by the enclosing lipid bilayer during enzymatic assays. Further, immobilization of HRP-containing LUV_{200} can be achieved via the vesicle membrane, *e.g. via* cholesterol tethers, leaving the enzyme uncompromised.66 HRP-encapsulating vesicles in combination with PPD and $ABTS^{2-}$ could potentially be used to monitor the integrity of surface bound vesicles. Additionally, compared to more conventional enzyme-based biosensors, lipid vesicles allow the study of membrane dependent events and biomolecules, e.g. solute permeation or ligand binding to membrane bound receptors.67 In both cases, HRP enclosed in the aqueous interior of lipid vesicles might act as sensitive reporter.

Supporting Information

Refer to Web version on PubMed Central for supplementary material.

Acknowledgments

The authors like to thank Prof. Dr. Stefanie D. Krämer, Dr. Reinhard Kissner, and Dr. Thomas Nauser for the discussions about vesicle permeability and about the oxidation of arylamines. Financial support by the Swiss National Foundation (Project Number 200020_150254), by the ERC Consolidator Grant (No. 681587, "HybCell" awarded to P.S.D.), the Graduate Student Innovation project (Grant KYLX-1140), and by the China Scholarship Council is greatly appreciated.

References

(1). Azevedo AM, Martin VC, Prazeres DMF, Vojinovic V, Cabral JMS, Fonseca LP. Biotechnol Annu Rev. 2003; 9:199–247. [PubMed: 14650928]

(2). Veitch NC. Phytochemistry. 2004; 65:249–259. [PubMed: 14751298]

(3). Dunford, HB. Peroxidases and Catalases. 2nd ed. Wiley; Hoboken, NJ: 2010.

(4). Torres, E., Ayala, M., editors. Biocatalysis Based on Heme Peroxidases: Peroxidases as Potential Industrial Biocatalysts. Springer; Berlin, Heidelberg, Germany: 2010.

(5). Ngo TT. Anal Lett. 2010; 43:1572–1587.

(6). Lopes GR, Pinto DCGA, Silva AMS. RSC Adv. 2014; 4:37244–37265.

(7). Krainer FW, Glieder A. Appl Microbiol Biotechnol. 2015; 99:1611–1625. [PubMed: 25575885]

(8). Childs RE, Bardsley WG. Biochem J. 1975; 145:93–103. [PubMed: 1191252]

(9). Scott SL, Chen W-J, Bakac A, Espenson JH. J Phys Chem. 1993; 97:6710–6714.

(10). Tarcha PJ, Chu VP, Whittern D. Anal Biochem. 1987; 165:230–233. [PubMed: 3688435]

(11). Fornera S, Walde P. Anal Biochem. 2010; 407:293–295. [PubMed: 20692226]

(12). Samygina VR, Sokolov AV, Bourenkov, Petoukhov MV 4, Pulina MO, Zakharova ET, Vasilyev VB, Bartunik H, Svergun DI. PLoS One. 2013; 8:e67145. [PubMed: 23843990]

(13). Rice EW. Anal Biochem. 1962; 3:452–456. [PubMed: 14491895]

(14). Sunderman FW, Nomoto S. Clin Chem. 1970; 16:903–910. [PubMed: 5473551]

(15). Lück, H. Methods of Enzymatic Analysis. 1st ed. Bergmeyer, HU., editor. Vol. 1. Academic Press; New York: 1963. p. 895-897. [It seems that after the initial suggestion for using PPD as HRP substrate, PPD was abandoned, most probably due to its oxidation by dioxygen (O_2), leading to non-negligible background reactions.]

(16). Aurand LW, Roberts WM, Cardwell JTJ. Dairy Sci. 1956; 39:568–573.

(17). Kokkinakis DM, Brooks JL. Plant Physiol. 1979; 63:93–99. [PubMed: 16660701]

(18). (a) The determined permeability coefficient for H_2O_2 for a POPC bilayer at 25 °C is about 10^{-4} cm/s: Yoshimoto M, Higa M. J Chem Technol Biotechnol. 2014; 89:1388–1395. This value compares with the determined permeability coefficient for H_2O for a POPC bilayer at 30 °C (≈ 1.3×10^{-2} cm/s): Mathai JC, Tristram-Nagle S, Nagle JF, Zeidel ML. J Gen Physiol. 2008; 131:69–76. [PubMed: 18166626]

(19). Bandrowski E. Ber Dtsch Chem Ges. 1894; 27:480–486.

(20). Corbett JF. J Chem Soc B. 1969:818–822.

(21). Blake AJ, Hubberstey P, Quinlan D. J Acta Crystallogr, Sect C: Cryst Struct Commun. 1996; 52:1774–1776.

(22). In this context it is worth noting that Jiao et al. demonstrated that PPD can be applied successfully as an electrochemical HRP substrate for a peroxidase-mediated voltammetric immunoassay, and that the reaction product is Bandrowski's base: Jiao K, Sun W, Zhang S-S, Sun G. Anal Chim Acta. 2000; 413:71–78.

(23). Haga M, Sugawara S, Itagaki H. Anal Biochem. 1981; 118:286–293. [PubMed: 7337225]

(24). Wu T-G, Durst RA. Microchim Acta. 1990; 100:187–195.

(25). Suita T, Tani H, Kamidate T. Anal Sci. 2000; 16:527–529.

(26). Hwang SY, Kumada Y, Seong GH, Choo J, Katoh S, Lee EK. Anal Bioanal Chem. 2007; 389:2251–2257. [PubMed: 17899025]

(27). Zheng Y, Chen H, Liu X-P, Jiang J-H, Luo Y, Shen GL, Yu R-Q. Talanta. 2008; 77:809–814.

(28). Banerjee J, Hanson AJ, Nyren-Erickson EK, Ganguli B, Wagh A, Muhonen WW, Law B, Shabb JB, Srivastava DK, Mallik S. Chem Commun. 2010; 46:3209–3211.

(29). Gomes MTR, Guimarães G, Frézard F, Kalapothakis E, Minozzo JC, Chaim OM, Veiga SS, Oliveira SC, Chévez-Olórtegui C. Toxicon. 2011; 57:574–579. [PubMed: 21236288]

(30). Genç R, Murphy D, Fragoso A, Ortiz M, O'Sullivan K. Anal Chem. 2011; 83:563–570. [PubMed: 21155541]

(31). Ge S, Jiao X, Chen D. Analyst. 2012; 137:4440–4447. [PubMed: 22866329]

(32). He Y, Li M, Jiang W, Yang WJ, Lin L, Xu LJ, Fu FF. J Mater Chem B. 2016; 4:752–759.

(33). Ren CD, Kurisawa M, Chung JE, Ying JY. J Mater Chem B. 2015; 3:4663–4670.

(34). Gupta N, Gupta C, Sharma S, Rathi B, Sharma RK, Bohidar HB. RSC Adv. 2016; 6:111099–111108.

(35). Kuiper SM, Nallani M, Vriezema DM, Cornelissen JJLM, van Hest JCM, Nolte RJM, Rowan AE. Org Biomol Chem. 2008; 6:4315–4318. [PubMed: 19005589]

(36). Spulber M, Najer A, Winkelbach K, Glaied O, Waser M, Pieles U, Meier W, Bruns NJ. Am Chem Soc. 2013; 135:9204–9212.

(37). Dinu MV, Spulber M, Renggli K, Wu D, Monnier CA, Petri-Fink A, Bruns N. Macromol Rapid Commun. 2015; 36:507–514. [PubMed: 25619496]

(38). Aibara S, Yamashita H, Mori E, Kato M, Morita Y. J Biochem. 1982; 92:531–539. [PubMed: 7130156]

(39). Mui B, Chow L, Hope MJ. Methods Enzymol. 2003; 367:3–14. [PubMed: 14611054]

(40). Suita T, Kamidate T, Yonaiyama M, Watanabe H. Anal Sci. 1997; 13:577–581.

(41). Blocher M, Walde P, Dunn IJ. Biotechnol Bioeng. 1999; 62:36–43. [PubMed: 10099511]

(42). Stewart JCM. Anal Biochem. 1980; 104:10–14. [PubMed: 6892980]

(43). Zuidam, J., de Vrueh, R., Crommelin, DJA. Liposomes: A Practical Approach. 2nd ed. Torchilin, V., Weissig, V., editors. Oxford University Press; Oxford UK: 2003. p. 31-78.

(44). Treyer M, Walde P, Oberholzer T. Langmuir. 2002; 18:1043–1050.

(45). Manoharan R, Dogra SK. Bull Chem Soc Jpn. 1987; 60:4409–4415.

(46). The reported pK_a value of the monoprotonated form of PPD is 6.10 (Manoharan and Dogra, 1987)45 or 6.44 (Corbett, 1969; Tong and Glesmann, 1964);20,47 the p*K*a value of the diprotonated PPD is about 2.4 (Manoharan and Dogra, 1987).45

(47). Tong LKJ, Glesmann C. Photogr Sci Eng. 1964; 8:319–325.

(48). Calculated from Figure 1 in the paper of Corbett (1969).20

(49). With $ABTS^{2-}$ as reducing substrate at pH = 7.0, a K_M value for H_2O_2 of (11.5 ± 1.1) μM was determined: Rodriguez-López JN, Smith AT, Thorneley RNF. J Biol Chem. 1996; 271:4023–4030. [PubMed: 8626735] Estimations based on kinetic measurements carried out at −26 °C in methanol/water mixtures yield a K_M value for H_2O_2 at 25 °C (pH = 7.3) of 46 μM: Baek HK, Van Wart EE. Biochemistry. 1989; 28:5714–5719. [PubMed: 2775733]

(50). Rodriguez-López JN, Gilabert MA, Tudela J, Thorneley RNF, García-Canovas F. Biochemistry. 2000; 39:13201–13209. [PubMed: 11052672]

(51). Ryabov AD, Goral VN, Gorton L, Csöregi E. Chem - Eur J. 1999; 5:961–967.

(52). Calculated from the data given in the footnote of Table 1 in Grotzky A, Altamura E, Adamcik J, Carrara P, Stano P, Mavelli F, Nauser T, Mezzenga R, Schlüter AD, Walde P. Langmuir. 2013; 29:10831–10840. [PubMed: 23895383]

(53). Yoshimoto M, Yamada J, Baba M, Walde P. ChemBioChem. 2016; 17:1221–1224. [PubMed: 27124158]

(54). Walde P, Ichikawa S. Biomol Eng. 2001; 18:143–177. [PubMed: 11576871]

(55). Inactivation of non-entrapped HRP by externally added proteinase K under nondenaturing conditions may not be successful, see Ghéczy N, Küchler A, Walde P. Anal Biochem. 2016; 513:54–60. [PubMed: 27594349]

(56). (a) Yoshimoto M, Miyazaki Y, Umemoto A, Walde P, Kuboi R, Nakao K. Langmuir. 2007; 23:9416–9422. [PubMed: 17655340] (b) Solís-Calero C, Ortega-Castro J, Muñoz F. J Phys Chem C. 2011; 115:22945–22953.

(57). The effect seems to be similar to the effect of tris(hydroxymethyl)aminomethane-buffer on the decomposition kinetics of peroxynitrite: Molina C, Kissner R, Koppenol WH. Dalton Trans. 2013; 42:9898–9905. [PubMed: 23698514]

(58). Frimer AA, Forman A, Borg DC. Isr J Chem. 1983; 23:442–445.

(59). Ullrich M, Hanuš J, Štěpánek F. Chem Eng Sci. 2015; 125:191–199.

(60). Tejwani RW, Anderson BD. J Pharm Sci. 2008; 97:381–399. [PubMed: 17694543]

(61). Cornell BA, Middlehurst J, Separovic F. Biochim Biophys Acta Biomembr. 1980; 598:405–410.

(62). Huang C, Mason JT. Proc Natl Acad Sci U S A. 1978; 75:308–310. [PubMed: 272647]

(63). The effect of the POPC LUV_{200} alone on the stability of PPD (see Figure S-13) has been neglected.

(64). Küchler A, Yoshimoto M, Luginbühl S, Mavelli F, Walde P. Nat Nanotechnol. 2016; 11:409–420. [PubMed: 27146955]

(65). Luna MA, Silber JJ, Sereno L, Correa NM, Moyano F. RSC Adv. 2016; 6:62594–62601.

(66). Kuhn P, Eyer K, Robinson T, Schmidt F, Mercer J, Dittrich PS. Integr Biol. 2012; 4:1550–1555.
(67). Christensen SM, Stamou DG. Sensors. 2010; 10:11352–11368. [PubMed: 22163531]

Europe PMC Funders Author Manuscripts

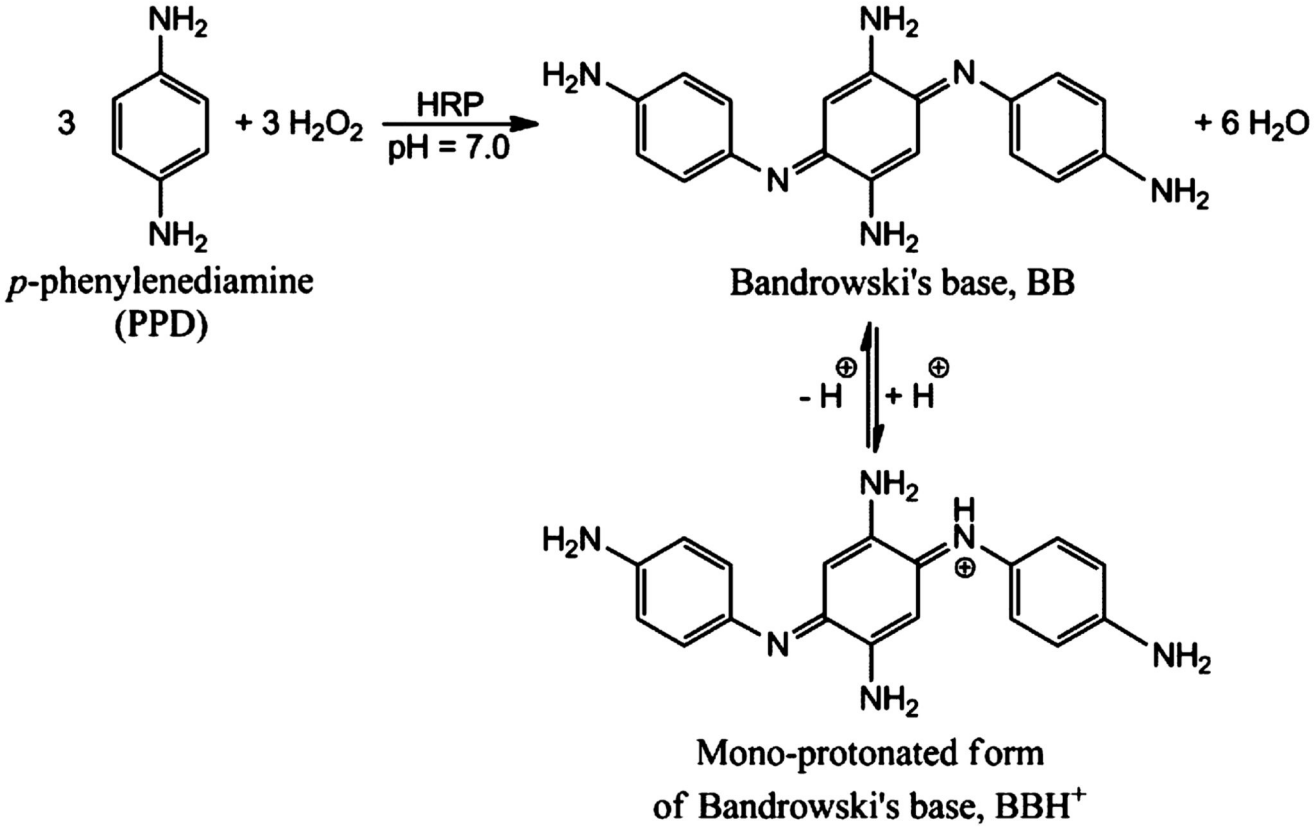

Figure 1.

Stoichiometric equation for the HRP-catalyzed oxidation of *p*-phenylenediamine (PPD) with H_2O_2 to Bandrowski's base at pH 7.0 in its neutral (BB) and monoprotonated (BBH^+) forms. The reported pK_a value of BBH^+ is 7.4.20 At pH 7.0, the calculated molar ratio of BBH^+ to BB is 2.5:1.

Europe PMC Funders Author Manuscripts

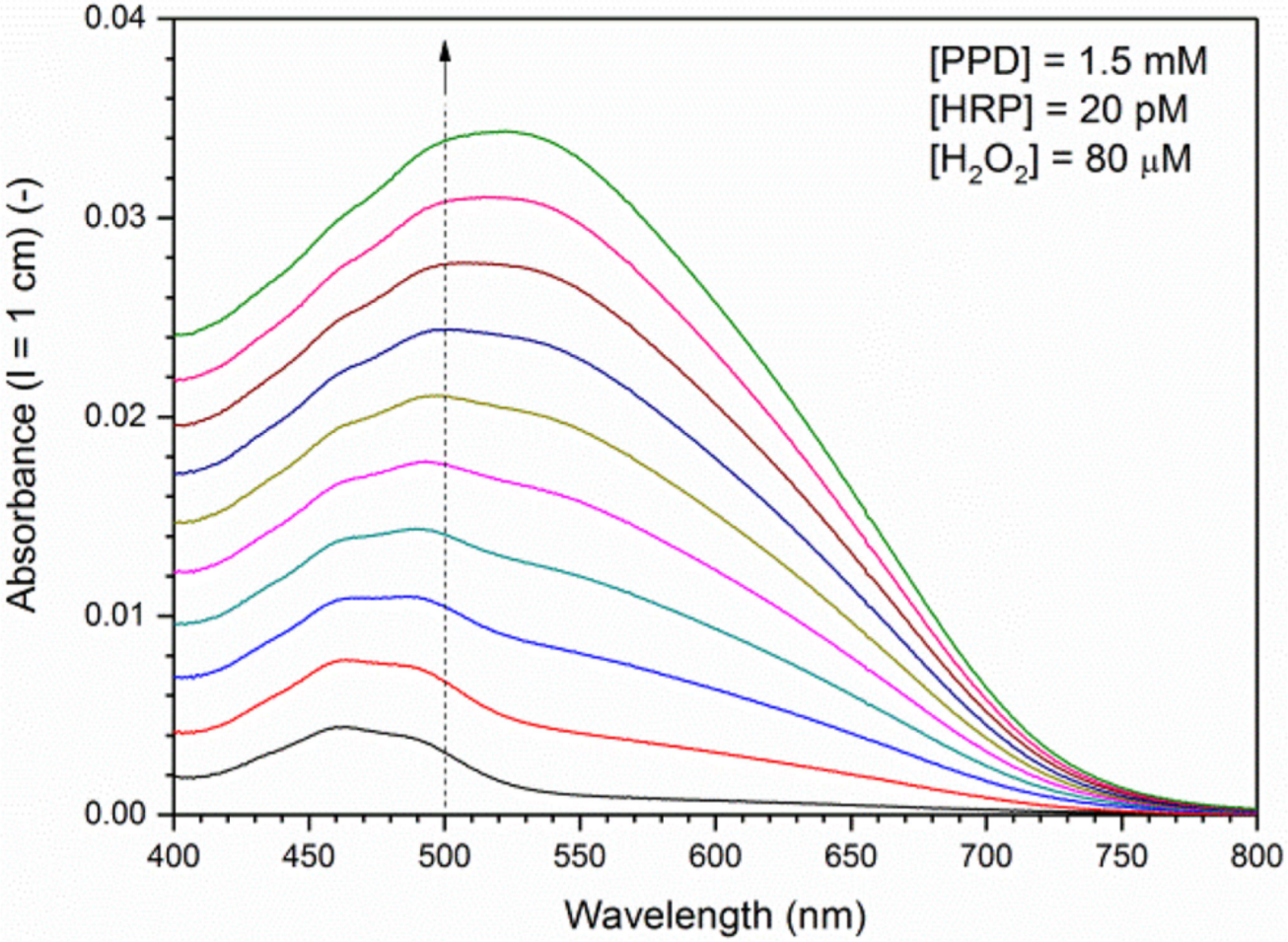

Figure 2.

Time-dependent changes in the absorption spectrum of a reaction solution which is kept at 25 °C containing initially 1.5 mM PPD, 20 pM HRP, and 80 μM H_2O_2 at pH 7.0 (buffer-1). The reaction solution was kept in a 1 cm quartz cell and the spectrum was recorded every min after starting the reaction by adding H_2O_2 for a total of 10 min. The dashed line indicates λ_{iso}; λ_{max} (BB) = 460 nm; λ_{max} (BBH^+) = 530−540 nm, see text for details. With ε_{500} = 1.109 × 10^4 M^{-1} cm^{-1} (see text), A_{500} (l = 1 cm) = 0.01 corresponds to 0.9 μM Bandrowski's base.

Europe PMC Funders Author Manuscripts

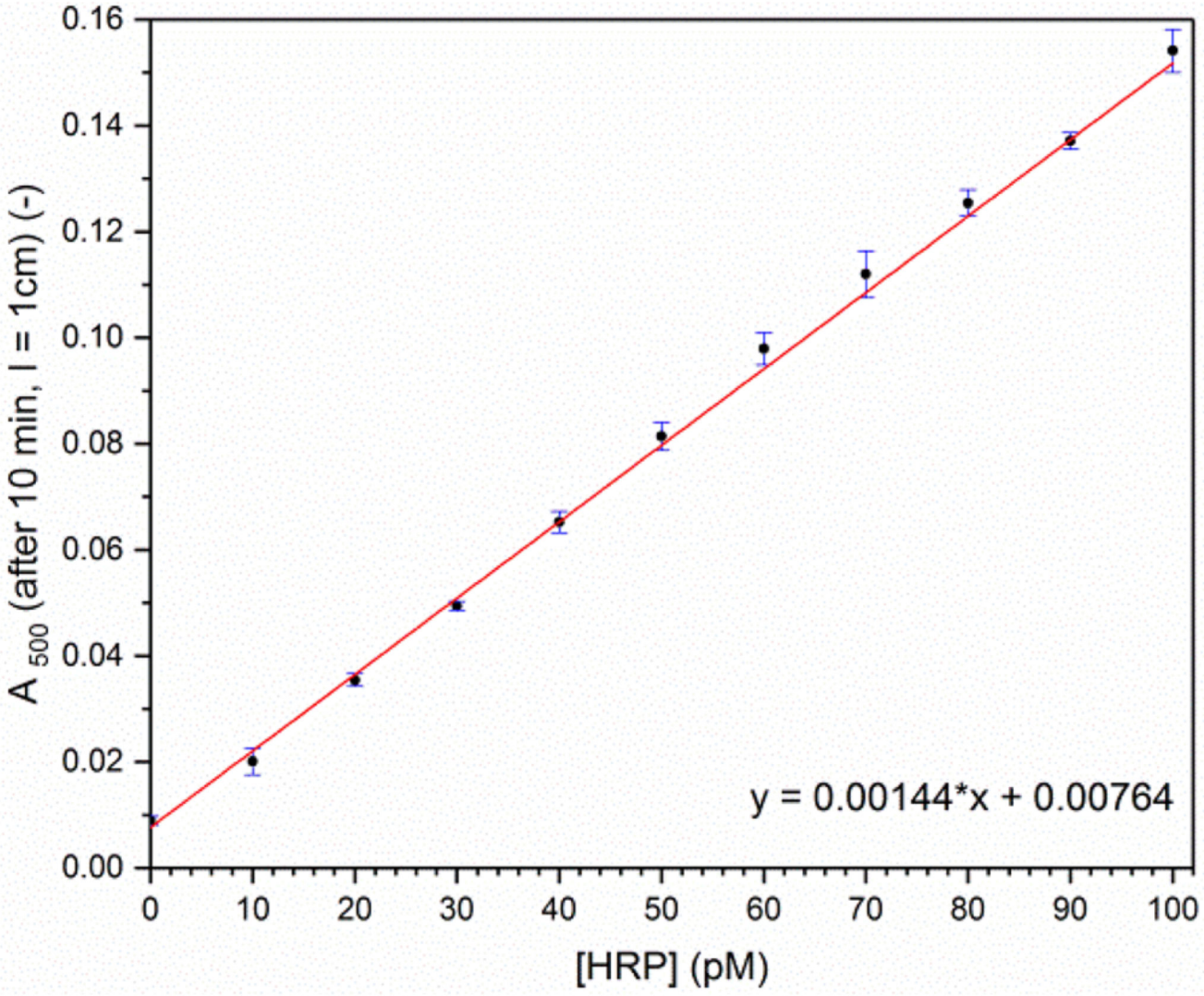

Figure 3.

HRP concentration dependency of the absorbance at 500 nm, A_{500}, measured after 10 min incubation at 25 °C for [PPD] = 1.5 mM, [H_2O_2] = 80 μM and pH 7.0 (buffer-1). Each data point represents the average and standard deviation for three measurements using the same HRP and H_2O_2 stock solutions and a freshly prepared PPD stock solution. Linear regression of the data points yields a slope of 0.00144 pM^{-1}, r^2 = 0.9993. With ε_{500} = 1.109 × 10^4 M^{-1} cm^{-1} (see text), A_{500} (l = 1 cm) = 0.10 corresponds to 9.0 μM Bandrowski's base.

Europe PMC Funders Author Manuscripts

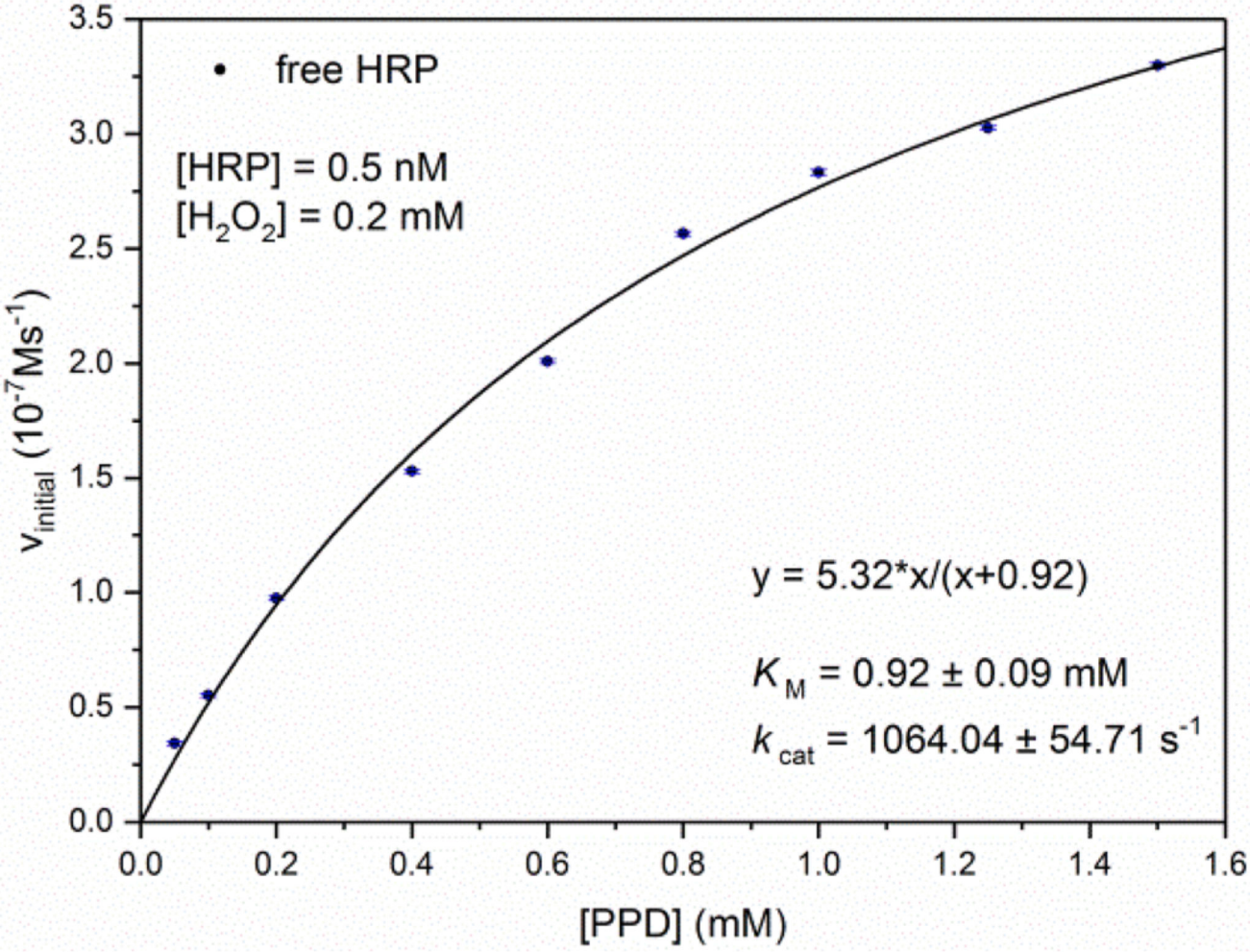

Figure 4.

HRP activity measurements with *p*-phenylenediamine (PPD) at 25 °C and pH = 7.0 (buffer-2), with 0.2 mM H_2O_2 and 0.5 nM HRP. The initial rate of product formation (Bandrowski's base) is plotted as a function of PPD concentration. Each data point represents the mean and standard deviation from three measurements. The data points were fit with the Michaelis−Menten equation, $r^2 = 0.9961$.

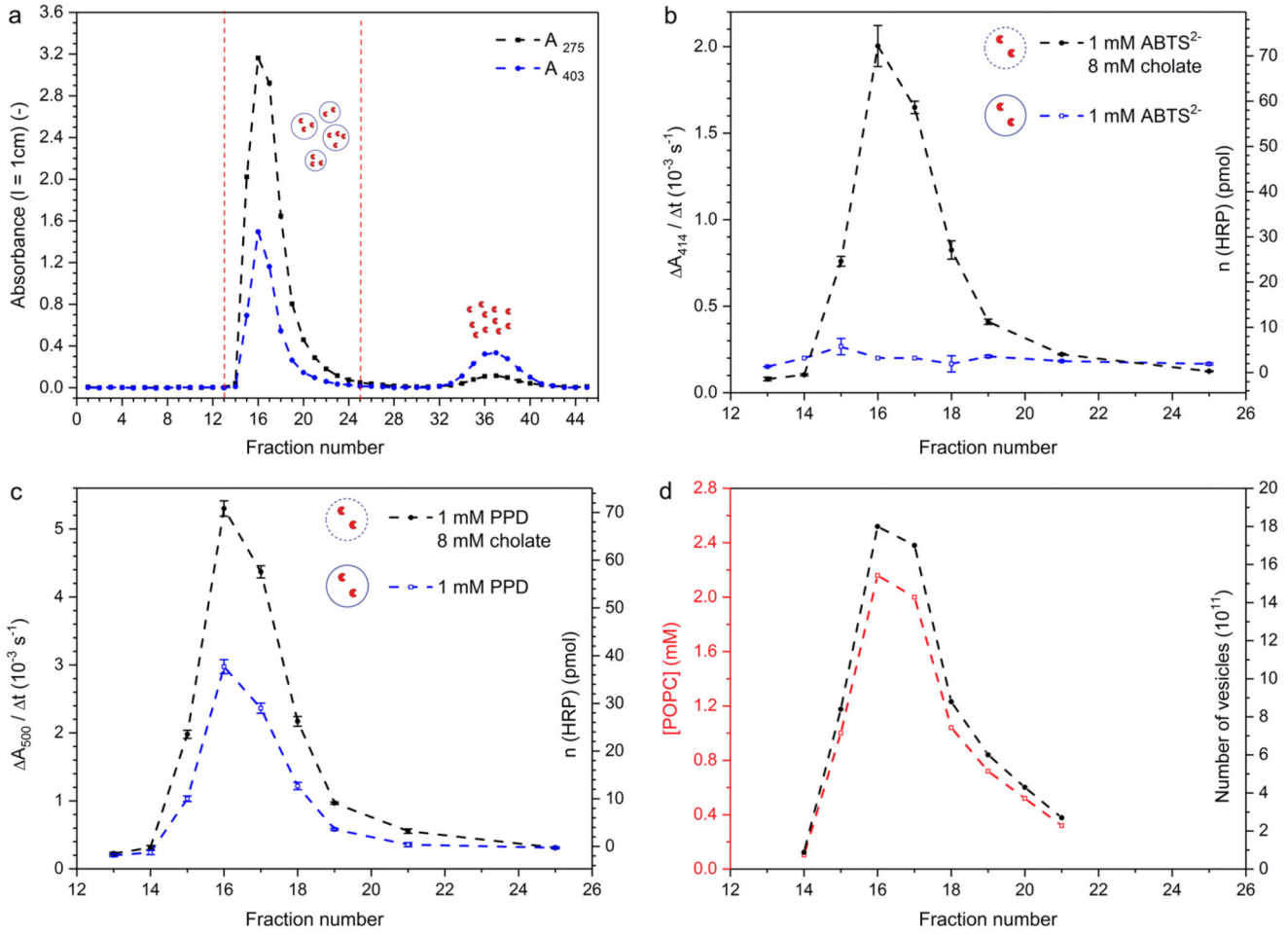

Figure 5.

Chromatogram for the separation of nonentrapped HRP from HRP-encapsulating POPC LUV_{200} by size exclusion chromatography with Sepharose 4B (l = 35 cm; d = 1.1 cm; applied volume, 0.5 mL (≈12 mM POPC, 31 μM HRP) (polycarbonate membrane extrusion resulted in a loss of POPC of ≈38%. Therefore, the POPC vesicle suspension applied onto the column had a concentration of ≈12 mM instead of 20 mM.); elution flow rate (buffer-2), 0.33 mL/min; fraction volume, 0.78 mL), see the Experimental Section for details. (a) A_{275} and A_{403} vs fraction number (l = 1 cm); (b and c) HRP activity measured with $ABTS^{2-}$ (b) or PPD (c) without (blue, open squares) and with cholate (8.0 mM, black, filled circles); the y-axis on the left-hand side is the increase in A_{414} (for $ABTS^{2-}$) or A_{500} (for PPD) per s, caused by the addition of 10 μL of the fraction to 1 mL of the assay solutions (l = 1 cm); the axis on the right-hand side refers to the calculated amount of HRP for the measurements carried out in the presence of 8.0 mM cholate and taking into account the calibration curves in Figure S-5b (for $ABTS^{2-}$) and Figure S-8b (for PPD); (d) POPC concentration, as determined with the Stewart assay and taking into account the calibration curve in Figure S-3 (left y-axis, red); the axis on the right-hand side refers to the calculated number of vesicles, see Table 1.

Europe PMC Funders Author Manuscripts

Europe PMC Funders Author Manuscripts

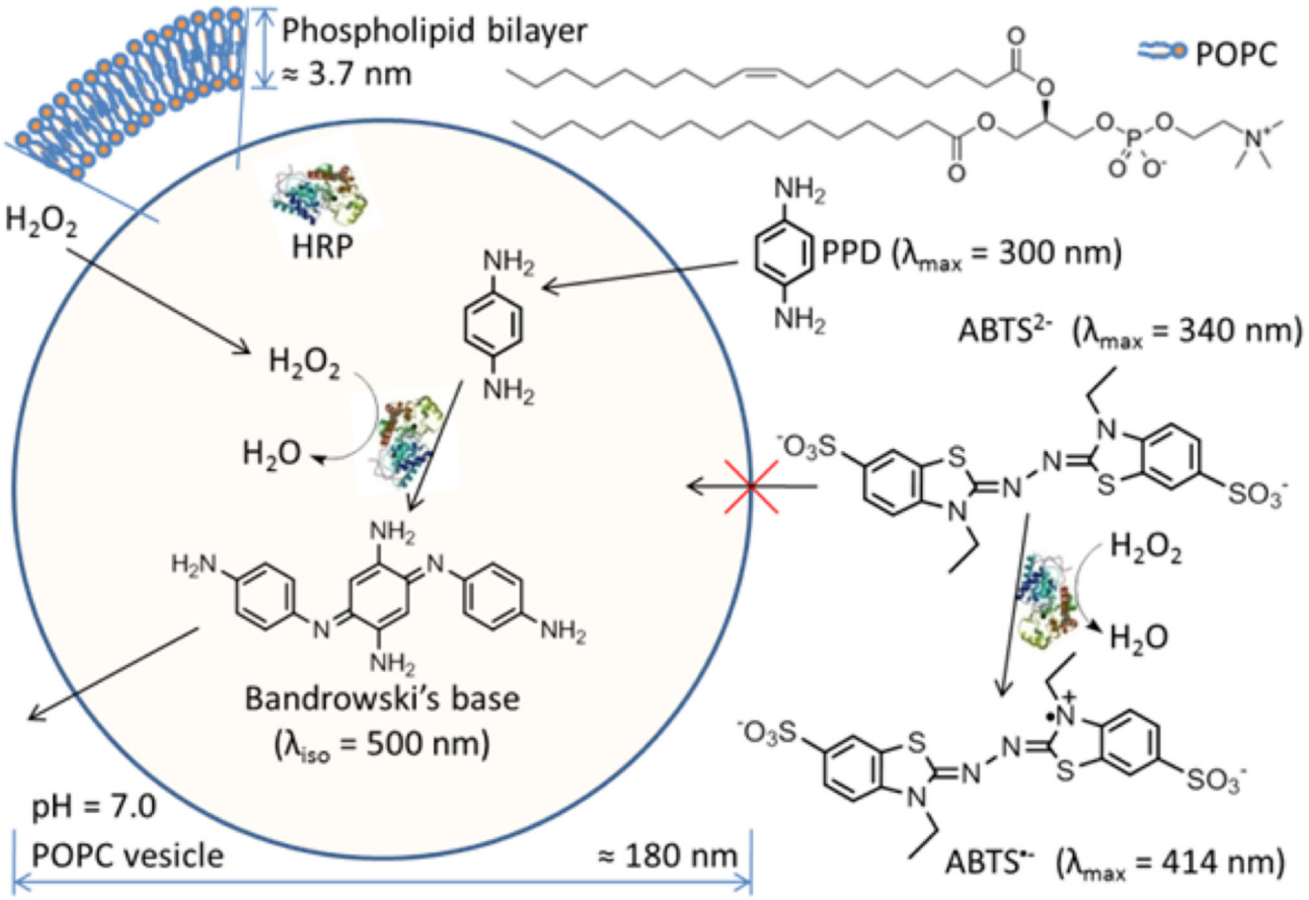

Figure 6.

Schematic representation of the selective oxidation of PPD in a suspension of HRP-encapsulating POPC LUV_{200} and externally added H_2O_2 and PPD or $ABTS^{2-}$. The cross-section of one spherical and unilamellar vesicle is shown. Since the POPC bilayer is permeable for H_2O_2 and PPD, but not for $ABTS^{2-}$, vesicle-trapped HRP can oxidize PPD (λ_{max} = 300 nm) to yield Bandrowski's base (λ_{iso} = 500 nm), while $ABTS^{2-}$ (λ_{max} = 340 nm) is only oxidized to $ABTS^{\bullet-}$ (λ_{max} = 414 nm) by HRP which is present in the bulk solution. The average size of one POPC vesicle is about 180 nm with a bilayer thickness of about 3.7 nm.

Europe PMC Funders Author Manuscripts

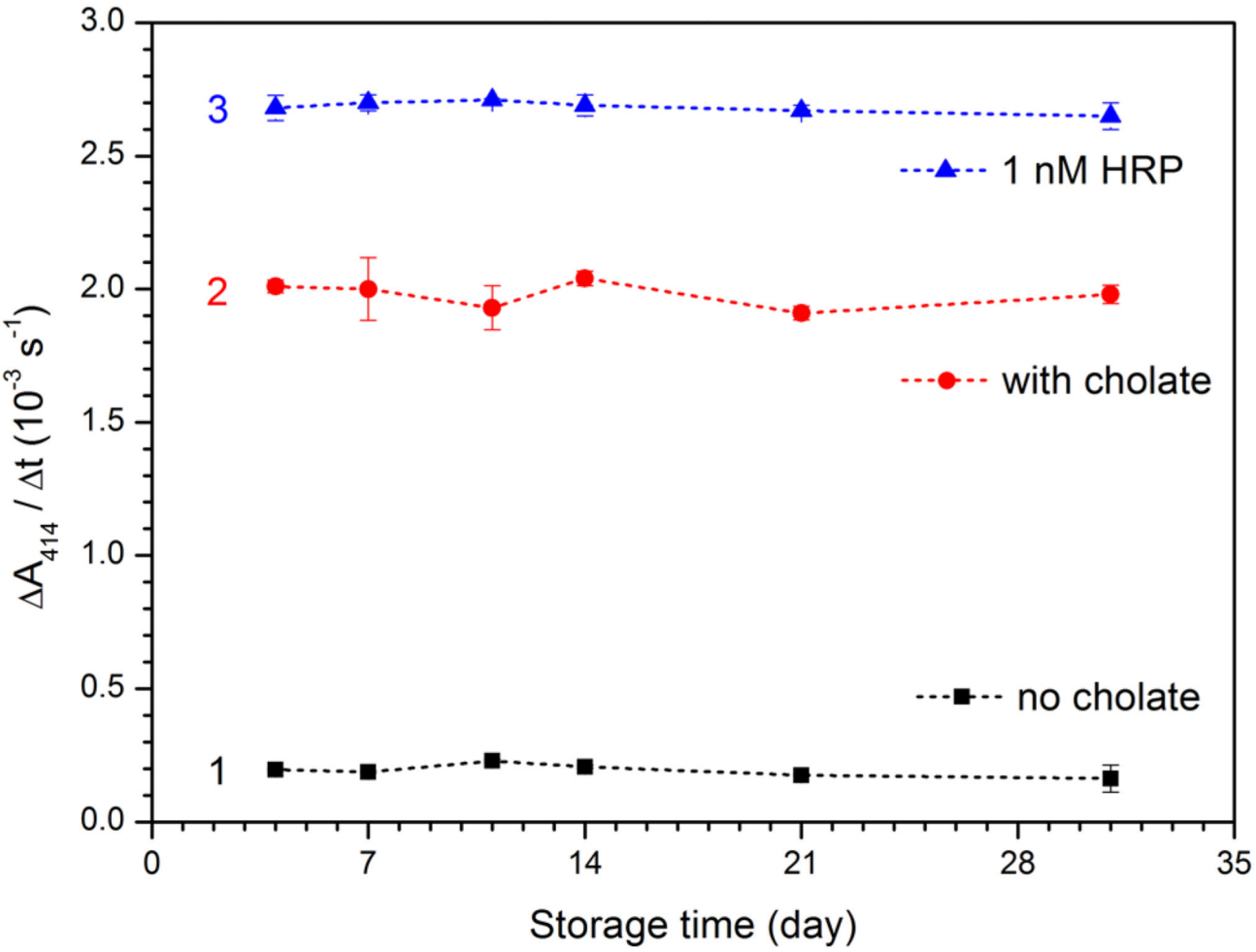

Figure 7.

Storage stability of HRP-encapsulating POPC vesicles (fraction 16, [POPC] = 2.17 mM, Figure 5), as determined with $ABTS^{2-}$ as the substrate and H_2O_2 as oxidant, either without added cholate for quantifying HRP which leaked from the vesicles into the bulk solution (black squares, 1) or after cholate was added (8.0 mM, red circles, 2) for quantifying the remaining total HRP activity after storage at 4 °C ($[HRP]_{overall}$ = 0.92 nM in the assay mixture). For a comparison, 1.4 nM HRP at pH 7.0 (buffer-2) was also stored at 4 °C and measured during 31 days (blue triangles, 3); the activity measurements were carried out at 25 °C with $[ABTS^{2-}]$ = 1.0 mM and $[H_2O_2]$ = 0.2 mM, [POPC] = 21.7 μM, see the Experimental Section for details. With $\varepsilon_{414} = 3.6 \times 10^4$ M^{-1} cm^{-1} (see text), $\Delta A_{414}/\Delta t$ (l = 1 cm) = 2.0×10^{-3} s^{-1} corresponds to 0.56 nM s^{-1} $ABTS^{\bullet-}$ formed.

Table 1

Characteristic Properties of the HRP-Encapsulating LUV_{200} Used in This Study

property	fractions 16	overall vesicle fraction [a]
[POPC]	2.17 mM	1.10 mM
n(POPC)	1.69 μmol	≈6.0 μmol
mean hydrodynamic vesicle diameter	180 nm	180 nm
POPC molecules per vesicle (N_{POPC})[b]	≈2.78×10^5	≈2.78×10^5
volume of one vesicle (V_{ves})	2.88×10^{-18} L	2.88×10^{-18} L
[vesicle][c]	7.8 nM	4.0 nM
number of vesicles (N_{ves})[d]	3.66×10^{12}	1.30×10^{13}
$[HRP]_{overall}$	92 nM	37 nM
n(HRP)	72 pmol	200 pmol
number of HRP molecules per vesicle (N_{HRP})[e]	≈12	≈9
$[HRP]_{inside}$ [f]	6.8 μM	5.3 μM

[a] Fractions 15–21 were considered. Each fraction had a volume of 0.78 mL; total volume of all vesicle fractions, 5.46 mL. Amounts applied onto the Sepharose 4B column, ≈6.0 μmol POPC (= 0.5 mL 12 μmol mL^{-1}) and ≈16 nmol HRP (= 0.5 mL 31 nmol mL^{-1}) (Figure 5).

[b] Calculated by assuming monodisperse, unilamellar and spherical vesicles. Further, a thickness of the POPC bilayer of 3.7 nm and a mean POPC headgroup area of 0.72 nm^2 were taken into account.61,62

[c] $[vesicle] = [POPC]/N_{POPC}$.

[d] $N_{ves} = n(POPC)N_A/N_{POPC}$; $N_A = 6.02 \times 10^{23}$, Avogadro's number.

[e] $N_{HRP} = n(HRP)N_A/N_{ves} = [HRP]_{overall}/[vesicle]$.

[f] $[HRP]_{inside} = n(HRP)/(V_{ves}N_{ves}) = N_{HRP}/(V_{ves}N_A)$.